Steel and Composite Structures, *Vol. 24, No. 1 (2017) 79-91*
DOI: https://doi.org/10.12989/scs.2017.24.1.079

Free vibration of a steel-concrete composite beam with coupled longitudinal and bending motions

Jun Li*, Li Jiang and Xiaobin Li

Departments of Naval Architecture, Ocean and Structural Engineering, School of Transportation, Wuhan University of Technology, Wuhan, China

(*Received September 18, 2016, Revised February 18, 2017, Accepted March 11, 2017*)

Abstract. Free vibrations of steel-concrete composite beams are analyzed by using the dynamic stiffness approach. The coupled equations of motion of the composite beams are derived with help of the Hamilton's principle. The effects of the shear deformation and rotary inertia of the two beams as well as the transverse and axial deformations of the stud connectors are included in the formulation. The dynamic stiffness matrix is developed on the basis of the exact general solutions of the homogeneous governing differential equations of the composite beams. The use of the dynamic stiffness method to determine the natural frequencies and mode shapes of a particular steel-concrete composite beam with various boundary conditions is demonstrated. The accuracy and effectiveness of the present model and formulation are validated by comparison of the present results with the available solutions in literature.

Keywords: steel-concrete composite beams; shear deformation; rotary inertia; free vibration; dynamic stiffness approach

1. Introduction

A particular target of interest in this paper is a steel-concrete composite beam. The configuration of this composite beam is composed of an upper beam made of concrete and a lower beam made of steel which is connected to the upper beam by a series of metallic studs. The two ends of the studs are embedded in the concrete slab and welded on the top surface of the steel beam, respectively. This kind of construction is broadly used in many engineering structures within the fields of bridge and building engineering due to its outstanding engineering properties such as high strength, high stiffness and high ductility.

Since the steel-concrete composite beams are often subjected to dynamic loads in complex environmental conditions, it is necessary to adopt an accurate mathematical model to analyze their vibration characteristics. Thus, the effects of the design parameters on the modal properties of the composite beams can be easily determined and can be used to improve the dynamic performance of the composite beams.

Because of the practical importance and potential benefits, there exists plenty of research concerning the various aspects of the steel-concrete composite beams. Among those investigations, the attention is greatly focused on the estimation of the static characteristics of the composite beams. A literature overview reveals that only a few researchers have made efforts to deal with the dynamic behavior of the composite beams.

Girhammar and Pan (1993) performed the exact and approximate dynamic analyses of the composite members with interlayer slip and attained the general closed-form solutions for the displacements and internal forces. Adam *et al*. (1997) investigated the flexural vibration of the elastic two-layer beams with interlayer slip using the Bernoulli-Euler beam theory and the linear constitutive equation between the horizontal slip and the interlaminar shear force. Using the Bernoulli-Euler beam theory Biscontin *et al*. (2000) proposed a one-dimensional model for the vibration analyses of steel-concrete composite beams, in which the same flexural displacement of the concrete slab and the steel beam was assumed and a strain energy density function was adopted to describe the stud connectors. Dilena and Morassi (2003) investigated the dynamic behavior of the steel-concrete composite beams with the damage in the junction, where the Bernoulli-Euler beam theory was used to construct the analytical model and the axial flexibility of the stud connectors was considered. Wu *et al*. (2007) investigated the free vibrations of the partial-interaction composite beams with axial force on the basis of the Bernoulli-Euler beam theory. Girhammar *et al*. (2009) treated the free and forced vibrations of the partial-interaction composite beams subjected to general dynamic loadings based on the Bernoulli-Euler beam theory. Shen *et al*. (2011) performed the dynamic analysis of the partial-interaction composite beams with generalized boundary conditions using the state-space method and Bernoulli-Euler beam theory. Li *et al*. (2014) analyzed the free vibration of the steel-concrete composite beams using the Bernoulli-Euler beam theory and dynamic stiffness method, in which the concrete slab and steel beam have the same transverse

*Corresponding author, Professor,
E-mail: LJY60023@yahoo.com

ISSN: 1229-9367 (Print), 1598-6233 (Online)

displacement and different longitudinal displacements. Berczynski and Wroblewski (2005) investigated the free vibrations of the steel-concrete composite beams using the Bernoulli-Euler beam theory and Timoshenko beam theory. The relative longitudinal and flexural displacements between the concrete slab and the steel beam were considered in the mathematical model. Xu and Wu (2007) studied the static, dynamic and buckling behavior of the partial-interaction composite beams with the shear deformation and rotary inertia of two beams taken into account. Dilena and Morassi (2009) presented a Bernoulli-Euler model and a Timoshenko model of steel-concrete composite beams and studied the vibration characteristics of the composite beams with partially degraded connection. Lenci and Clementi (2012) studied the linear dynamics of a two-layer beam with normal and tangential detachments where each beam was modeled by the Timoshenko kinematics and all inertia terms were considered. Based on the two-dimensional theory of elasticity, Xu and Wu (2008) adopted the state-space method conjunction with the differential quadrature method to study the free vibration and buckling behavior of the partial-interaction composite beams with axial force. Henderson *et al*. (2015b) simulated the dynamic behavior of the steel-concrete composite beams using the model based on the Timoshenko beam theory, in which the relative longitudinal and transverse displacements between the steel beam and the concrete slab were considered. Nguyen *et al*. (2012) presented an exact analysis approach for the free vibration of two-layer shear-deformable beams by assuming that the two layers had the same transverse displacement and the negligible rotary inertias. Zhou *et al*. (2016) presented the analytical solution of the free flexural vibration of the steel-composite composite beams based on the Timoshenko beam theory with the transverse separation between the concrete slab and the steel beam ignored. Morassi and Rocchetto (2003) conducted the experimental tests on four steel-concrete composite beams and examined the effect of the damage formed in the connection on the natural frequency and mode shape. Berczynski and Wroblewski (2010) carried out the experimental study to validate the natural vibration models of the steel-concrete composite beams. Henderson *et al*. (2015a) performed an experimental study on three steel-concrete composite beams with different shear connection types. Morassi *et al*. (2005, 2007) and Jimbo *et al*. (2012) applied the dynamic analysis of steel-composite beams to identify the possible damage inside the connection.

In order to accurately evaluate the modal characteristics of the steel-concrete composite beams, a comprehensive structural model must be employed. It is well-known that due to the neglect of the transverse shear effect the elementary Bernoulli-Euler beam theory may increase the displacement and decrease the natural frequency. As a result, the Timoshenko beam theory that considers the effects of shear deformation and rotary inertia is adopted in this paper, which will more satisfactorily approximate the dynamic behavior of the composite beams. The finite rigidity of the connection provided by the stud connectors between the concrete slab and the steel beam makes the dynamic behavior of composite beams more complex. The effect of the stud connectors is described by their strain energy, which considers the transverse and axial deformations of the studs. The main task of this paper is to develop an exact dynamic stiffness matrix for a steel-concrete composite beam. The dynamic stiffness method used to determine the natural frequencies and mode shapes has certain advantages over the conventional finite element and other approximate methods, because it is based on the closed-form analytical solutions of the homogeneous governing differential equations. Therefore, the dynamic stiffness method allows an infinite number of modal properties of a vibrating structure to be accounted for, without loss of accuracy.

This paper deals with the development and solution of the equations of motion governing the free vibration of the steel-concrete composite beams. The coupled governing differential equations of motion of the composite beams are derived using the Hamilton's principle. The exact general solutions of the homogeneous governing equations of motion are employed to formulate the dynamic stiffness matrix, which represents the relationship of the generalized forces and generalized displacements at the two ends of the composite beams. The modal properties of the steel-concrete composite beams with any desired boundary conditions can be computed by using the corresponding stiffness terms of the dynamic stiffness matrix. The Wittrick-Williams algorithm (Wittrick and Williams 1971) is adopted together with the dynamic stiffness matrix to determine the eigenfrequencies of a particular steel-concrete composite beam. The accuracy and effectiveness of the present model and formulation are demonstrated and the influence due to boundary condition on the eigen-frequencies of the appropriately chosen example is presented.

2. Mathematical model

The longitudinal and transverse vibrations of a composite beam system in the o_1xz_1 plane as shown in Fig. 1 are investigated. The system consists of an upper beam made of concrete and a lower beam made of steel which is

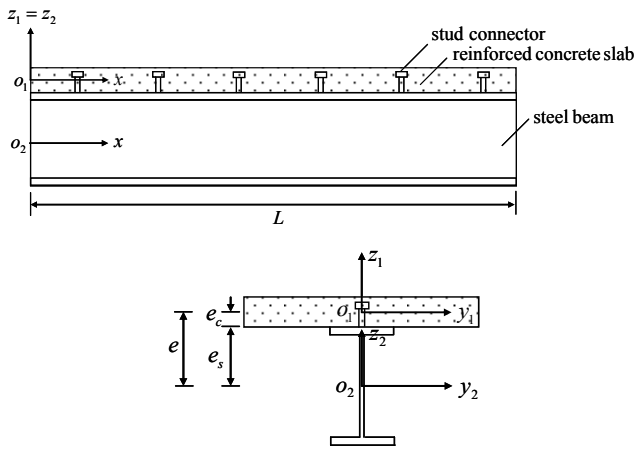

Fig. 1 Configuration of a steel-concrete composite beam

connected to the upper beam by a series of metallic connectors or studs. The top ends and bottom ends of the connectors are embedded in the concrete slab and welded on the top surface of the steel beam, respectively.

The basic assumptions used to derive the governing differential equations of motion of the steel-concrete composite beam are described as follows:

(1) Both the concrete slab and the steel beam are homogeneous, prismatic and of the same length L;
(2) The materials of the concrete slab and steel beam behave linear elastic and isotropic;
(3) The Timoshenko beam theory applies to the concrete slab and steel beam;
(4) The relative slide between the concrete slab and the steel beam occurs on the contact interface and the relative transverse displacement occurs between the concrete slab and the steel beam;
(5) The connectors or studs are uniformly distributed longitudinally; the distance between the two consecutive connectors is small when compared with the beam length L and the length of the connectors is half of the thickness of the concrete slab.

Since the effects of the shear deformation and rotary inertia of the concrete slab and steel beam are allowed for, the total kinetic energy T and strain energy V of the concrete slab and steel beam can be given by

$$\begin{aligned} T = {} & 1/2\int_0^L m_1\left[(\dot{u}_1)^2+(\dot{w}_1)^2\right]dx + 1/2\int_0^L \rho_1 I_1(\dot{\psi}_1)^2 dx \\ & + 1/2\int_0^L m_2\left[(\dot{u}_2)^2+(\dot{w}_2)^2\right]dx + 1/2\int_0^L \rho_2 I_2(\dot{\psi}_2)^2 dx \end{aligned} \tag{1}$$

$$\begin{aligned} V = {} & 1/2\int_0^L k_1 G_1 A_1\left(w_1'-\psi_1\right)^2 dx + 1/2\int_0^L E_1 I_1\left(\psi_1'\right)^2 dx \\ & + 1/2\int_0^L E_1 A_1\left(u_1'\right)^2 dx + 1/2\int_0^L k_2 G_2 A_2\left(w_2'-\psi_2\right)^2 dx \\ & + 1/2\int_0^L E_2 I_2\left(\psi_2'\right)^2 dx + 1/2\int_0^L E_2 A_2\left(u_2'\right)^2 dx \end{aligned} \tag{2}$$

where $u_i = u_i(x, t)$, $w_i = w_i(x, t)$ and $\psi_i = \psi_i(x, t)$ (i = 1, 2) are the longitudinal displacement, transverse displacement and normal rotation of the concrete slab and steel beam, respectively. x and t are the spatial coordinate and the time, respectively. E_i, G_i, ρ_i and m_i are the Young's modulus, shear modulus, mass density per unit volume and mass density per unit length of the concrete slab and steel beam, respectively. A_i, I_i and k_i are the cross-sectional area, second moment of area and shear correction factor of the concrete slab and steel beam, respectively. The subscripts 1 and 2 are used to distinguish the quantities relevant to the concrete slab and steel beam. The superscripts prime and overdot indicate the partial differentiation with respect to the coordinate x and time t, respectively.

The relative longitudinal displacement and relative transverse displacement can occur between the concrete slab and the steel beam. However, these relative displacements are constrained by the connectors which produce a series of concentrated forces and moments acting on the concrete slab and steel beam at their junctions with the connectors. The strain energy of the ith connector can be defined as (Berczynski and Wroblewski 2005)

$$\begin{aligned} V_{ci} = {} & 1/2\left[1/2\,Ke_c(\zeta_1+\zeta_2)+K\delta_1\right]\delta_1 \\ & + 1/2\left[1/6\,Ke_c^2(2\zeta_1+\zeta_2)+1/2\,Ke_c\delta_1\right]\zeta_1 \\ & + 1/2\left[1/6\,Ke_c^2(\zeta_1+2\zeta_2)+1/2\,Ke_c\delta_1\right]\zeta_2 \\ & + 1/2\left(E_cA_c/e_c\,\delta_2\right)\delta_2 \end{aligned} \tag{3}$$

where K, E_c and A_c denote the shear stiffness, Young's modulus and cross-sectional area of the connector, respectively. $\zeta_1 = \psi_1$ and $\zeta_2 = \psi_2$ denote the top end rotation and bottom end rotation of the connector, respectively. It should be mentioned that the top end and bottom end of the connector are fixed to the neutral axis of the concrete slab and the upper surface of the steel beam, respectively. $\delta_1 = u_2 - u_1 = \psi_2 e_s$ and $\delta_1 = w_1 - w_2$ denote the relative transverse displacement and relative longitudinal displacement between the top end and the bottom end of the connector, respectively. e_c and e_s are the distance between the top surface of the steel beam and the centroid of the concrete slab and the distance between the top surface of the steel beam and the centroid of the steel beam, respectively, as shown in Fig. 1.

Substituting the expressions of ζ_1, ζ_2, δ_1 and δ_2 into Eq. (3) and conducting some algebraic manipulations result in

$$\begin{aligned} V_{ci} = {} & 1/2\,Ke_c(u_2-u_1+\psi_2e_s)\psi_1 \\ & + 1/2\,Ke_c(u_2-u_1+\psi_2e_s)\psi_2 \\ & + 1/2\,K(u_2-u_1+\psi_2e_s)^2 \\ & + 1/6\,Ke_c^2\left[(\psi_1)^2+\psi_1\psi_2+(\psi_2)^2\right] \\ & + 1/2\,E_cA_c/e_c\,(w_1-w_2)^2 \end{aligned} \tag{4}$$

On the basis of assumption (5) the discrete connectors can be approximated as the continuous connection. Thus, the strain energy of all the connectors is simply described as

$$V_c = \int_0^L \begin{Bmatrix} 1/2\,ke_c(u_2-u_1+\psi_2e_s)\psi_1 \\ +1/2\,ke_c(u_2-u_1+\psi_2e_s)\psi_2 \\ +1/2\,k(u_2-u_1+\psi_2e_s)^2 \\ +1/6\,ke_c^2\left[(\psi_1)^2+\psi_1\psi_2+(\psi_2)^2\right] \\ +1/2\,\mu(w_1-w_2)^2 \end{Bmatrix} \tag{5}$$

where $k = K/d$ and $\mu = e_cA_c/e_cd$ are the shear stiffness and axial stiffness per unit length of the connection, respectively. d is the distance between the two consecutive connectors.

The governing differential equations of motion and the associated boundary conditions of the steel-concrete composite beam can be derived conveniently with help of the Hamilton's principle, which may be stated in the form

$$\begin{aligned} & \int_{t_1}^{t_2}\delta(T-V-V_c)dt = 0 \\ & \delta u_1 = \delta w_1 = \delta\psi_1 = \delta u_2 = \delta w_2 = \delta\psi_2 = 0 \quad \text{at} \quad t = t_1, t_2 \end{aligned} \tag{6}$$

where δ denotes the variation calculus.

Substitution of Eqs. (1), (2) and (5) into Eq. (6) and integrating by parts yield the following governing differential equations of motion of the steel-concrete composite beam

$$\begin{aligned}&-m_1\ddot{u}_1+E_1A_1u_1''-ku_1+1/2\,ke_c\psi_1\\&+ku_2+\left(1/2\,ke_c+ke_s\right)\psi_2=0\end{aligned}\tag{7a}$$

$$-m_1\ddot{w}_1+k_1G_1A_1w_1''-\mu w_1-k_1G_1A_1\psi_1'+\mu w_2=0\tag{7b}$$

$$\begin{aligned}&-\rho_1I_1\ddot{\psi}_1+1/2\,ke_cu_1+k_1G_1A_1w_1'+E_1I_1\psi_1''\\&-\left(k_1G_1A_1+1/3\,ke_c^2\right)\psi_1-1/2\,ke_cu_2\\&-\left(1/6\,ke_c^2+1/2\,ke_ce_s\right)\psi_2=0\end{aligned}\tag{7c}$$

$$\begin{aligned}&-m_2\ddot{u}_2+ku_1-1/2\,ke_c\psi_1+E_2A_2u_2''-ku_2\\&-\left(1/2\,ke_c+ke_s\right)\psi_2=0\end{aligned}\tag{7d}$$

$$-m_2\ddot{w}_2+\mu w_1+k_2G_2A_2w_2''-\mu w_2-k_2G_2A_2\psi_2'=0\tag{7e}$$

$$\begin{aligned}&-\rho_2I_2\ddot{\psi}_2+\left(1/2\,ke_c+ke_s\right)u_1-\left(1/6\,ke_c^2+1/2\,ke_ce_s\right)\psi_1\\&-\left(1/2\,ke_c+ke_s\right)u_2+k_2G_2A_2w_2'+E_2I_2\psi_2''\\&-\left(k_2G_2A_2+1/3\,ke_c^2+ke_ce_s+ke_s^2\right)\psi_2=0\end{aligned}\tag{7f}$$

The associated boundary conditions at the composite beam ends ($x = 0, L$) are

$$u_1=0\quad\text{or}\quad N_1=E_1A_1u_1'\tag{8a}$$

$$w_1=0\quad\text{or}\quad S_1=-\left(k_1G_1A_1w_1'-k_1G_1A_1\psi_1\right)\tag{8b}$$

$$\psi_1=0\quad\text{or}\quad M_1=-E_1I_1\psi_1'\tag{8c}$$

$$u_2=0\quad\text{or}\quad N_2=E_2A_2u_2'\tag{8d}$$

$$w_2=0\quad\text{or}\quad S_2=-\left(k_2G_2A_2w_2'-k_2G_2A_2\psi_2\right)\tag{8e}$$

$$\psi_2=0\quad\text{or}\quad M_2=-E_2I_2\psi_2'\tag{8f}$$

3. Dynamic stiffness formulation

If the steel-concrete composite beam vibrates freely, the axial displacement u_i, the transverse displacement w_i and the normal rotation ψ_i can be expressed as

$$\begin{aligned}&\left\{u_1(x,t)\ w_1(x,t)\ \psi_1(x,t)\ u_2(x,t)\ w_2(x,t)\ \psi_2(x,t)\right\}\\&=\left\{U_1(x)\ W_1(x)\ \Psi_1(x)\ U_2(x)\ W_2(x)\ \Psi_2(x)\right\}e^{i\omega t}\end{aligned}\tag{9}$$

where ω is the circular frequency, $U_i(x)$, $W_i(x)$ and $\Psi_i(x)$ describe the mode functions of the sinusoidally varying axial displacement, transverse displacement and normal rotation, respectively.

Substitution of Eq. (9) into Eqs. (7a)-(7f) and eliminating the time-dependent term yield

$$a_1U_1''+a_2U_1+a_3\Psi_1+kU_2+a_4\Psi_2=0\tag{10a}$$

$$a_5W_1''+a_6W_1-a_5\Psi_1'+\mu W_2=0\tag{10b}$$

$$a_3U_1+a_5W_1'+a_7\Psi_1''+a_8\Psi_1-a_3U_2-a_9\Psi_2=0\tag{10c}$$

$$kU_1-a_3\Psi_1+a_{10}U_2''+a_{11}U_2-a_4\Psi_2=0\tag{10d}$$

$$\mu W_1+a_{12}W_2''+a_{13}W_2-a_{12}\Psi_2'=0\tag{10e}$$

$$a_4U_1-a_9\Psi_1-a_4U_2+a_{12}W_2'+a_{14}\Psi_2''+a_{15}\Psi_2=0\tag{10f}$$

where

$$\begin{gathered}a_1=E_1A_1\qquad a_2=m_1\omega^2-k\qquad a_3=1/2\,ke_c\\a_4=1/2\,ke_c+ke_s\qquad a_5=k_1G_1A_1\qquad a_6=m_1\omega^2-\mu\\a_7=E_1I_1\qquad a_8=\rho_1I_1\omega^2-\left(k_1G_1A_1+1/3\,ke_c^2\right)\\a_9=1/6\,ke_c^2+1/2\,ke_ce_s\qquad a_{10}=E_2A_2\\a_{11}=m_2\omega^2-k\qquad a_{12}=k_2G_2A_2\\a_{13}=m_2\omega^2-\mu\qquad a_{14}=E_2I_2\\a_{15}=\rho_2I_2\omega^2-\left(k_2G_2A_2+1/3\,ke_c^2+ke_ce_s+ke_s^2\right)\end{gathered}$$

Since Eqs. (10a)-(10f) are a set of ordinary differential equations with constant coefficients, the displacement and rotation mode functions $U_i(x)$, $W_i(x)$ and $\Theta_i(x)$ can be assumed to have the following forms

$$\begin{aligned}&\left\{U_1(x)\ W_1(x)\ \Psi_1(x)\ U_2(x)\ W_2(x)\ \Psi_2(x)\right\}\\&=\left\{\widetilde{A}\ \widetilde{B}\ \widetilde{C}\ \widetilde{D}\ \widetilde{E}\ \widetilde{F}\right\}e^{\kappa x}\end{aligned}\tag{11}$$

Substituting Eqs. (11) into Eqs. (10a)-(10f) and letting the determinant of the coefficient matrix of $\widetilde{A}$, $\widetilde{B}$, $\widetilde{C}$, $\widetilde{D}$, $\widetilde{E}$ and $\widetilde{F}$ equal to zero produce the characteristics equation, which is an twelfth-order polynomial equation in κ

$$\eta_6\kappa^{12}+\eta_5\kappa^{10}+\eta_4\kappa^8+\eta_3\kappa^6+\eta_2\kappa^4+\eta_1\kappa^2+\eta_0=0\tag{12}$$

where the coefficients η_i ($i = 0 – 6$) are described in detail in the Appendix.

The general solutions to Eqs. (10a)-(10f) take the forms of

$$U_1(x)=\sum_{j=1}^{6}\left(\overline{A}_{2j-1}e^{\kappa_jx}+\overline{A}_{2j}e^{-\kappa_jx}\right)\tag{13a}$$

$$W_1(x)=\sum_{j=1}^{6}\left(\overline{B}_{2j-1}e^{\kappa_jx}+\overline{B}_{2j}e^{-\kappa_jx}\right)\tag{13b}$$

$$\Psi_1(x)=\sum_{j=1}^{6}\left(\overline{C}_{2j-1}e^{\kappa_jx}+\overline{C}_{2j}e^{-\kappa_jx}\right)\tag{13c}$$

$$U_2(x)=\sum_{j=1}^{6}\left(\overline{D}_{2j-1}e^{\kappa_jx}+\overline{D}_{2j}e^{-\kappa_jx}\right)\tag{13d}$$

$$W_2(x)=\sum_{j=1}^{6}\left(\overline{E}_{2j-1}e^{\kappa_jx}+\overline{E}_{2j}e^{-\kappa_jx}\right)\tag{13e}$$

$$\Psi_2(x)=\sum_{j=1}^{6}(\overline{F}_{2j-1}e^{\kappa_j x}+\overline{F}_{2j}e^{-\kappa_j x}) \tag{13f}$$

where $\kappa_j=\sqrt{\chi_j}$ (j = 1 – 6), χ_j are the roots of the following sixth-order polynomial equation

$$\eta_6\chi^6+\eta_5\chi^5+\eta_4\chi^4+\eta_3\chi^3+\eta_2\chi^2+\eta_1\chi+\eta_0=0 \tag{14}$$

In the solution of Eq. (14), if any of the χ_j's are zero or are repeated, the solutions to Eqs. (10a)-(10f) will be modified according to the well-known methods for the ordinary differential equations with constant coefficients, for those particular values of χ_j.

In Eqs. (13a)-(13f) $\overline{A}_1-\overline{A}_{12}$, $\overline{B}_1-\overline{B}_{12}$, $\overline{C}_1-\overline{C}_{12}$, $\overline{D}_1-\overline{D}_{12}$, $\overline{E}_1-\overline{E}_{12}$ and $\overline{F}_1-\overline{F}_{12}$ are six sets of twelve constants. However, there are only twelve independent constants. Introducing Eqs. (13a)-(13f) into Eqs. (10a)-(10e) obtains the relations between the constants

$$\overline{A}_{2j-1}=t_j\overline{B}_{2j-1} \qquad \overline{A}_{2j}=-t_j\overline{B}_{2j} \tag{15a}$$

$$\overline{C}_{2j-1}=\bar{t}_j\overline{B}_{2j-1} \qquad \overline{C}_{2j}=-\bar{t}_j\overline{B}_{2j} \tag{15b}$$

$$\overline{D}_{2j-1}=\hat{t}_j\overline{B}_{2j-1} \qquad \overline{D}_{2j}=-\hat{t}_j\overline{B}_{2j} \tag{15c}$$

$$\overline{E}_{2j-1}=\tilde{t}_j\overline{B}_{2j-1} \qquad \overline{E}_{2j}=\tilde{t}_j\overline{B}_{2j} \tag{15d}$$

$$\overline{F}_{2j-1}=\breve{t}_j\overline{B}_{2j-1} \qquad \overline{F}_{2j}=-\breve{t}_j\overline{B}_{2j} \tag{15e}$$

where the coefficients t_j, $\bar{t}_j$, $\hat{t}_j$, $\tilde{t}_j$ and $\breve{t}_j$ (j = 1 – 6) are presented in the Appendix.

In view of the sign convention shown in Fig. 2 and removing the time-dependent term, the expressions of the amplitude functions $N_1(x)$, $N_2(x)$, $S_2(x)$, $M_1(x)$, $M_2(x)$ of the sinusoidally varying normal forces, shear forces and bending moments for the steel-concrete composite beam can be written from Eqs. (8a)-(8f), (13a)-(13f) and (15a)-(15e), respectively, as follows

$$\begin{aligned}N_1(x)&=a_1U_1'\\&=\sum_{j=1}^{6}a_1t_j\kappa_j(\overline{B}_{2j-1}e^{\kappa_j x}+\overline{B}_{2j}e^{-\kappa_j x})\end{aligned} \tag{16a}$$

$$\begin{aligned}S_1(x)&=-\left(a_5W_1'-a_5\Psi_1\right)\\&=\sum_{j=1}^{6}\left(-a_5\kappa_j+a_5\bar{t}_j\right)(\overline{B}_{2j-1}e^{\kappa_j x}-\overline{B}_{2j}e^{-\kappa_j x})\end{aligned} \tag{16b}$$

$$\begin{aligned}M_1(x)&=-a_7\Psi_1'\\&=\sum_{j=1}^{6}-a_7\bar{t}_j\kappa_j(\overline{B}_{2j-1}e^{\kappa_j x}+\overline{B}_{2j}e^{-\kappa_j x})\end{aligned} \tag{16c}$$

$$\begin{aligned}N_2(x)&=a_{10}U_2'\\&=\sum_{j=1}^{6}a_{10}\hat{t}_j\kappa_j(\overline{B}_{2j-1}e^{\kappa_j x}+\overline{B}_{2j}e^{-\kappa_j x})\end{aligned} \tag{16d}$$

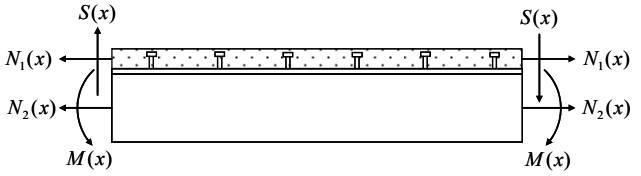

Fig. 2 Sign convention for positive normal forces $N_1(x)$, $N_2(x)$, shear forces $S_1(x)$, $S_2(x)$ and bending moments $M_1(x)$, $M_2(x)$

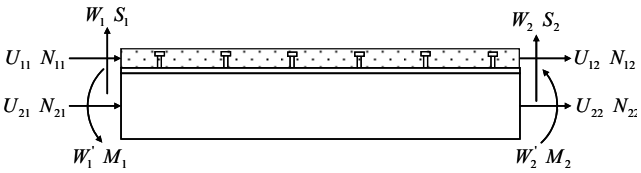

Fig. 3 Boundary conditions for generalized displacements and generalized forces of steel-concrete composite beam

$$\begin{aligned}S_2(x)&=-\left(a_{12}W_2'-a_{12}\Psi_2\right)\\&=\sum_{j=1}^{6}\left(-a_{12}\tilde{t}_j\kappa_j+a_{12}\breve{t}_j\right)(\overline{B}_{2j-1}e^{\kappa_j x}-\overline{B}_{2j}e^{-\kappa_j x})\end{aligned} \tag{16e}$$

$$\begin{aligned}M_2(x)&=-a_{14}\Psi_2'\\&=\sum_{j=1}^{6}-a_{14}\breve{t}_j\kappa_j(\overline{B}_{2j-1}e^{\kappa_j x}+\overline{B}_{2j}e^{-\kappa_j x})\end{aligned} \tag{16f}$$

With reference to Fig. 3, the boundary conditions for the generalized displacements and generalized forces of the steel-concrete composite beam are, respectively,

Displacements

$$\begin{aligned}\text{At } x=0:\ &U_1=U_{11} \quad W_1=W_{11} \quad \Psi_1=\Psi_{11}\\&U_2=U_{21} \quad W_2=W_{21} \quad \Psi_2=\Psi_{21}\end{aligned} \tag{17a}$$

$$\begin{aligned}\text{At } x=L:\ &U_1=U_{12} \quad W_1=W_{12} \quad \Psi_1=\Psi_{12}\\&U_2=U_{22} \quad W_2=W_{22} \quad \Psi_2=\Psi_{22}\end{aligned} \tag{17b}$$

Forces

$$\begin{aligned}\text{At } x=0:\ &N_1=-N_{11} \quad S_1=S_{11} \quad M_1=M_{11}\\&N_2=-N_{21} \quad S_2=S_{21} \quad M_2=M_{21}\end{aligned} \tag{17c}$$

$$\begin{aligned}\text{At } x=L:\ &N_1=N_{12} \quad S_1=-S_{12} \quad M_1=-M_{12}\\&N_2=N_{22} \quad S_2=-S_{22} \quad M_2=-M_{22}\end{aligned} \tag{17d}$$

Substituting Eqs. (17a) and (17b) into Eqs. (13a)-(13f) and taking into account Eqs. (15a)-(15e), the nodal displacements at the steel-concrete composite beam ends, shown in Fig. 3, can be expressed by the twelve constants $\overline{B}_{2j}(\overline{B}_{2j-1})$ (j = 1 – 6) as

$$\{D\} = [R]\{\overline{B}\} \tag{18}$$

where $\{D\}$ is the nodal degree-of-freedom vector defined by

$$\{D\} = \{U_{11}\ W_{11}\ \Psi_{11}\ U_{21}\ W_{21}\ \Psi_{21}\ U_{12}\ W_{12}\ \Psi_{12}\ U_{22}\ W_{22}\ \Psi_{22}\}^T$$

$\{\overline{B}\}$ is composed of the twelve constants $\overline{B}_{2j}(\overline{B}_{2j-1})$ (j = 1 – 6) as follows

$$\{\overline{B}\} = \{\overline{B}_1\ \overline{B}_3\ \overline{B}_5\ \overline{B}_7\ \overline{B}_9\ \overline{B}_{11}\ \overline{B}_2\ \overline{B}_4\ \overline{B}_6\ \overline{B}_8\ \overline{B}_{10}\ \overline{B}_{12}\}^T$$

$$[R] = \begin{bmatrix}
t_1 & t_2 & t_3 & t_4 & t_5 & t_6 \\
1 & 1 & 1 & 1 & 1 & 1 \\
\bar{t}_1 & \bar{t}_2 & \bar{t}_3 & \bar{t}_4 & \bar{t}_5 & \bar{t}_6 \\
\hat{t}_1 & \hat{t}_2 & \hat{t}_3 & \hat{t}_4 & \hat{t}_5 & \hat{t}_6 \\
\tilde{t}_1 & \tilde{t}_2 & \tilde{t}_3 & \tilde{t}_4 & \tilde{t}_5 & \tilde{t}_6 \\
\breve{t}_1 & \breve{t}_2 & \breve{t}_3 & \breve{t}_4 & \breve{t}_5 & \breve{t}_6 \\
t_1e^{\kappa_1 L} & t_2e^{\kappa_2 L} & t_3e^{\kappa_3 L} & t_4e^{\kappa_4 L} & t_5e^{\kappa_5 L} & t_6e^{\kappa_6 L} \\
e^{\kappa_1 L} & e^{\kappa_2 L} & e^{\kappa_3 L} & e^{\kappa_4 L} & e^{\kappa_5 L} & e^{\kappa_6 L} \\
\bar{t}_1e^{\kappa_1 L} & \bar{t}_2e^{\kappa_2 L} & \bar{t}_3e^{\kappa_3 L} & \bar{t}_4e^{\kappa_4 L} & \bar{t}_5e^{\kappa_5 L} & \bar{t}_6e^{\kappa_6 L} \\
\hat{t}_1e^{\kappa_1 L} & \hat{t}_2e^{\kappa_2 L} & \hat{t}_3e^{\kappa_3 L} & \hat{t}_4e^{\kappa_4 L} & \hat{t}_5e^{\kappa_5 L} & \hat{t}_6e^{\kappa_6 L} \\
\tilde{t}_1e^{\kappa_1 L} & \tilde{t}_2e^{\kappa_2 L} & \tilde{t}_3e^{\kappa_3 L} & \tilde{t}_4e^{\kappa_4 L} & \tilde{t}_5e^{\kappa_5 L} & \tilde{t}_6e^{\kappa_6 L} \\
\breve{t}_1e^{\kappa_1 L} & \breve{t}_2e^{\kappa_2 L} & \breve{t}_3e^{\kappa_3 L} & \breve{t}_4e^{\kappa_4 L} & \breve{t}_5e^{\kappa_5 L} & \breve{t}_6e^{\kappa_6 L}
\end{bmatrix}$$

$$\begin{bmatrix}
-t_1 & -t_2 & -t_3 & -t_4 & -t_5 & -t_6 \\
1 & 1 & 1 & 1 & 1 & 1 \\
-\bar{t}_1 & -\bar{t}_2 & -\bar{t}_3 & -\bar{t}_4 & -\bar{t}_5 & -\bar{t}_6 \\
-\hat{t}_1 & -\hat{t}_2 & -\hat{t}_3 & -\hat{t}_4 & -\hat{t}_5 & -\hat{t}_6 \\
\tilde{t}_1 & \tilde{t}_2 & \tilde{t}_3 & \tilde{t}_4 & \tilde{t}_5 & \tilde{t}_6 \\
-\breve{t}_1 & -\breve{t}_2 & -\breve{t}_3 & -\breve{t}_4 & -\breve{t}_5 & -\breve{t}_6 \\
-t_1e^{-\kappa_1 L} & -t_2e^{-\kappa_2 L} & -t_3e^{-\kappa_3 L} & -t_4e^{-\kappa_4 L} & -t_5e^{-\kappa_5 L} & -t_6e^{-\kappa_6 L} \\
e^{-\kappa_1 L} & e^{-\kappa_2 L} & e^{-\kappa_3 L} & e^{-\kappa_4 L} & e^{-\kappa_5 L} & e^{-\kappa_6 L} \\
-\bar{t}_1e^{-\kappa_1 L} & -\bar{t}_2e^{-\kappa_2 L} & -\bar{t}_3e^{-\kappa_3 L} & -\bar{t}_4e^{-\kappa_4 L} & -\bar{t}_5e^{-\kappa_5 L} & -\bar{t}_6e^{-\kappa_6 L} \\
-\hat{t}_1e^{-\kappa_1 L} & -\hat{t}_2e^{-\kappa_2 L} & -\hat{t}_3e^{-\kappa_3 L} & -\hat{t}_4e^{-\kappa_4 L} & -\hat{t}_5e^{-\kappa_5 L} & -\hat{t}_6e^{-\kappa_6 L} \\
\tilde{t}_1e^{-\kappa_1 L} & \tilde{t}_2e^{-\kappa_2 L} & \tilde{t}_3e^{-\kappa_3 L} & \tilde{t}_4e^{-\kappa_4 L} & \tilde{t}_5e^{-\kappa_5 L} & \tilde{t}_6e^{-\kappa_6 L} \\
-\breve{t}_1e^{-\kappa_1 L} & -\breve{t}_2e^{-\kappa_2 L} & -\breve{t}_3e^{-\kappa_3 L} & -\breve{t}_4e^{-\kappa_4 L} & -\breve{t}_5e^{-\kappa_5 L} & -\breve{t}_6e^{-\kappa_6 L}
\end{bmatrix}$$

Inserting Eqs. (17c) and (17d) into Eqs. (16a)-(16f) and consideration of Eqs. (15a)-(15e), the nodal forces corresponding to the twelve nodal displacements, as exhibited in Fig. 3, also can be described in terms of the twelve constants $\overline{B}_{2j}(\overline{B}_{2j-1})$ (j = 1 – 6) as

$$\{F\} = [H]\{\overline{B}\} \tag{19}$$

where $\{F\}$ is the nodal force vector indicated by

$$\{F\} = \{N_{11}\ S_{11}\ M_{11}\ N_{21}\ S_{21}\ M_{21}\ N_{12}\ S_{12}\ M_{12}\ N_{22}\ S_{22}\ M_{22}\}^T$$

$$[H] = \begin{bmatrix}
-\hat{\hat{t}}_1 & -\hat{\hat{t}}_2 & -\hat{\hat{t}}_3 & -\hat{\hat{t}}_4 & -\hat{\hat{t}}_5 & -\hat{\hat{t}}_6 \\
\tilde{\tilde{t}}_1 & \tilde{\tilde{t}}_2 & \tilde{\tilde{t}}_3 & \tilde{\tilde{t}}_4 & \tilde{\tilde{t}}_5 & \tilde{\tilde{t}}_6 \\
\hat{\tilde{t}}_1 & \hat{\tilde{t}}_2 & \hat{\tilde{t}}_3 & \hat{\tilde{t}}_4 & \hat{\tilde{t}}_5 & \hat{\tilde{t}}_6 \\
-\tilde{\tilde{t}}_1 & -\tilde{\tilde{t}}_2 & -\tilde{\tilde{t}}_3 & -\tilde{\tilde{t}}_4 & -\tilde{\tilde{t}}_5 & -\tilde{\tilde{t}}_6 \\
\hat{\breve{t}}_1 & \hat{\breve{t}}_2 & \hat{\breve{t}}_3 & \hat{\breve{t}}_4 & \hat{\breve{t}}_5 & \hat{\breve{t}}_6 \\
\tilde{\breve{t}}_1 & \tilde{\breve{t}}_2 & \tilde{\breve{t}}_3 & \tilde{\breve{t}}_4 & \tilde{\breve{t}}_5 & \tilde{\breve{t}}_6 \\
\hat{\hat{t}}_1e^{\kappa_1 L} & \hat{\hat{t}}_2e^{\kappa_2 L} & \hat{\hat{t}}_3e^{\kappa_3 L} & \hat{\hat{t}}_4e^{\kappa_4 L} & \hat{\hat{t}}_5e^{\kappa_5 L} & \hat{\hat{t}}_6e^{\kappa_6 L} \\
-\tilde{\tilde{t}}_1e^{\kappa_1 L} & -\tilde{\tilde{t}}_2e^{\kappa_2 L} & -\tilde{\tilde{t}}_3e^{\kappa_3 L} & -\tilde{\tilde{t}}_4e^{\kappa_4 L} & -\tilde{\tilde{t}}_5e^{\kappa_5 L} & -\tilde{\tilde{t}}_6e^{\kappa_6 L} \\
-\hat{\hat{t}}_1e^{\kappa_1 L} & -\hat{\hat{t}}_2e^{\kappa_2 L} & -\hat{\hat{t}}_3e^{\kappa_3 L} & -\hat{\hat{t}}_4e^{\kappa_4 L} & -\hat{\hat{t}}_5e^{\kappa_5 L} & -\hat{\hat{t}}_6e^{\kappa_6 L} \\
\tilde{\tilde{t}}_1e^{\kappa_1 L} & \tilde{\tilde{t}}_2e^{\kappa_2 L} & \tilde{\tilde{t}}_3e^{\kappa_3 L} & \tilde{\tilde{t}}_4e^{\kappa_4 L} & \tilde{\tilde{t}}_5e^{\kappa_5 L} & \tilde{\tilde{t}}_6e^{\kappa_6 L} \\
\hat{\tilde{t}}_1e^{\kappa_1 L} & \hat{\tilde{t}}_2e^{\kappa_2 L} & \hat{\tilde{t}}_3e^{\kappa_3 L} & \hat{\tilde{t}}_4e^{\kappa_4 L} & \hat{\tilde{t}}_5e^{\kappa_5 L} & \hat{\tilde{t}}_6e^{\kappa_6 L} \\
-\tilde{\breve{t}}_1e^{\kappa_1 L} & -\tilde{\breve{t}}_2e^{\kappa_2 L} & -\tilde{\breve{t}}_3e^{\kappa_3 L} & -\tilde{\breve{t}}_4e^{\kappa_4 L} & -\tilde{\breve{t}}_5e^{\kappa_5 L} & -\tilde{\breve{t}}_6e^{\kappa_6 L} \\
-\hat{\hat{t}}_1e^{-\kappa_1 L} & -\hat{\hat{t}}_2e^{-\kappa_2 L} & -\hat{\hat{t}}_3e^{-\kappa_3 L} & -\hat{\hat{t}}_4e^{-\kappa_4 L} & -\hat{\hat{t}}_5e^{-\kappa_5 L} & -\hat{\hat{t}}_6e^{-\kappa_6 L} \\
\tilde{\tilde{t}}_1e^{-\kappa_1 L} & \tilde{\tilde{t}}_2e^{-\kappa_2 L} & \tilde{\tilde{t}}_3e^{-\kappa_3 L} & \tilde{\tilde{t}}_4e^{-\kappa_4 L} & \tilde{\tilde{t}}_5e^{-\kappa_5 L} & \tilde{\tilde{t}}_6e^{-\kappa_6 L} \\
\hat{\tilde{t}}_1e^{-\kappa_1 L} & \hat{\tilde{t}}_2e^{-\kappa_2 L} & \hat{\tilde{t}}_3e^{-\kappa_3 L} & \hat{\tilde{t}}_4e^{-\kappa_4 L} & \hat{\tilde{t}}_5e^{-\kappa_5 L} & \hat{\tilde{t}}_6e^{-\kappa_6 L} \\
-\tilde{\breve{t}}_1e^{-\kappa_1 L} & -\tilde{\breve{t}}_2e^{-\kappa_2 L} & -\tilde{\breve{t}}_3e^{-\kappa_3 L} & -\tilde{\breve{t}}_4e^{-\kappa_4 L} & -\tilde{\breve{t}}_5e^{-\kappa_5 L} & -\tilde{\breve{t}}_6e^{-\kappa_6 L}
\end{bmatrix}$$

in which

$$\hat{\hat{t}}_j = a_1 t_j \kappa_j \qquad \tilde{\tilde{t}}_j = -a_5\kappa_j + a_5\bar{t}_j \qquad \hat{\tilde{t}}_j = -a_7\bar{t}_j\kappa_j$$
$$\tilde{\breve{t}}_j = a_{10}\hat{t}_j\kappa_j \qquad \breve{\tilde{t}}_j = -a_{12}\tilde{t}_j\kappa_j + a_{12}\breve{t}_j \qquad \tilde{\tilde{t}}_j = -a_{14}\breve{t}_j\kappa_j$$
$$(j = 1-6)$$

The dynamic stiffness equation can be generated by combining Eqs. (18) and (19) and eliminating the constant vector $\{\overline{B}\}$, which is given by

$$\{F\} = [\overline{K}]\{D\} \tag{20}$$

where $[\overline{K}] = [H][R]^{-1}$ is the exact dynamic stiffness matrix of the steel-concrete composite beam. It may be mentioned that dynamic stiffness matrix is symmetric and frequency-dependent.

The derived element dynamic stiffness matrix can be directly applied to a single-span steel-concrete composite beam with various boundary conditions. If a structure composed of steel-concrete composite beams is investigated, the element dynamic stiffness matrix can be assembled in the same way as that used for the classical finite element method to construct the total dynamic stiffness matrix of the structure. Because the dynamic stiffness formulation leads to a transcendental eigenvalue problem, some elegant solution techniques must be adopted in order to ensure that no natural frequencies of the structure being analyzed are missed. In the present study,

Table 1 Eigenfrequencies (in Hz) of the steel-concrete composite beam

Mode No.	C-C	C-H1	C-H2	F-F			C-F	H1-H1	H2-H2
				Present	Berczynski and Wroblewski (2005)	Biscontin *et al*. (2000)			
1	50.44	44.71	37.54	58.22	58.339	59.625	9.62	39.94	26.03
2	121.33	109.35	105.77	138.21	138.870	133.875	52.78	98.60	90.41
3	213.41	196.57	194.97	236.61	238.015	235.250	129.75	180.67	176.98
4	321.07	300.84	300.18	347.93	350.042	345.000	224.73	281.24	279.70
5	441.57	418.76	309.32	470.49	473.104	459.000	309.32	396.44	395.77
6	572.70	547.72	418.47	602.24	605.115	578.250	334.48	523.19	522.89
7	617.68	617.67	547.59	617.70*	N/A	617.750*	456.00	617.67	617.67
8	713.17	686.09	686.02	742.32	745.216	706.750	587.54	659.49	659.35
9	862.41	833.12	833.09	890.14	892.908	853.000	727.78	804.37	804.30
10	1020.58	988.88	924.32	1046.66	N/A	N/A	876.37	957.79	957.75
11	1188.16	1153.91	988.86	1211.78	N/A	N/A	924.38	1120.29	1120.28
12	1228.88	1288.88	1153.90	1229.29*	N/A	1233.625*	1033.70	1228.87	1228.88
13	1365.80	1328.91	1328.91	1388.21	N/A	N/A	1200.35	1292.66	1292.65
14	1553.96	1514.49	1514.48	1584.52	N/A	N/A	1376.94	1475.61	1475.60

*Note: The superscript asterisk denotes the longitudinal vibration mode

a reliable and accurate method, i.e., the well-known Wittrick-Williams algorithm (Wittrick and Williams 1971), is employed together with the dynamic stiffness matrix to determine the natural frequencies of the steel-concrete composite beam or its assembly. This algorithm uses the Sturm sequence property of the dynamic stiffness matrix and finds the total number of the natural frequencies below an arbitrarily chosen trial value rather than directly calculating the natural frequencies. The application of the algorithm when using the dynamic stiffness formulation has been discussed in a large number of papers (e.g., Lee 2009) and is not explained here for brevity. The mode shapes corresponding to the natural frequencies can be found in the usual way by making an arbitrary assumption about one appropriately chosen and unknown variable of the steel-concrete composite beam system and then calculating the remaining variables in terms of the appropriately chosen one.

4. Numerical results and discussion

Application of the dynamic stiffness formulation derived above to the study of free vibration of a particular steel-concrete composite beam is carried out. The natural frequencies and mode shapes of the composite beam are determined to assess the accuracy and effectiveness of the proposed formulation. The effect of the boundary condition upon the natural frequencies of the composite beam is also presented. Four types of supports at the beam end are under investigation. These are

(1) Clamped support (C):

$$U_1 = W_1 = \Psi_1 = U_2 = W_2 = \Psi_2 = 0$$

(2) Hinged support 1 (H1):

$$U_1 = W_1 = M_1 = U_2 = W_2 = M_2 = 0$$

(3) Hinged support 2 (H2):

$$N_1 = W_1 = M_1 = N_2 = W_2 = M_2 = 0$$

(4) Free support (F):

$$N_1 = S_1 = M_1 = N_2 = S_2 = M_2 = 0$$

The concerned composite beam consists of an upper concrete slab having a depth of 0.06 m and a width of 0.5 m and a lower steel beam made of a Fe430 steel section bar of IPE 140 series. The concrete slab is connected to the steel beam by a group of studs made of Fe430 steel. The diameter of the studs equals to 0.0125 m and the ends of studs are embedded in the concrete slab and welded on the top flange of the steel beam. The Young's modulus E_2, cross-sectional area A_2 and moment of inertia J_2 of the steel beam as well as the cross-sectional area A_1 and moment of inertia J_1 of the concrete slab are assumed to equal to their nominal values. The mass densities per unit volume ρ_i and mass densities per unit length m_i of the concrete slab and steel beam are extracted from the measurement of the total mass of each beam in the event of homogeneous material. The Young's modulus E_1 of the concrete slab and the shear stiffness K of each stud are usually deduced with help of the experimental tests. The Young's modulus E_c and cross-sectional area A_c of each stud are chosen as its nominal values. The shear modulus G_i of the concrete slab and steel beam can be obtained using the relation $G_i = E_i/2(1+\nu_i)$, where ν_i is the Poisson ratio of the concrete and steel. The shear correction factor k_i of the concrete slab and steel beam can be estimated by the formula (Berczynski and Wroblewski 2005) $k_i = (A_i S_i^2)\int_{A_i} (\tau_{xyi}^2 + \tau_{xzi}^2) dA_i$, in which τ_{xyi} and τ_{xzi} denote the shear stresses of the concrete slab and

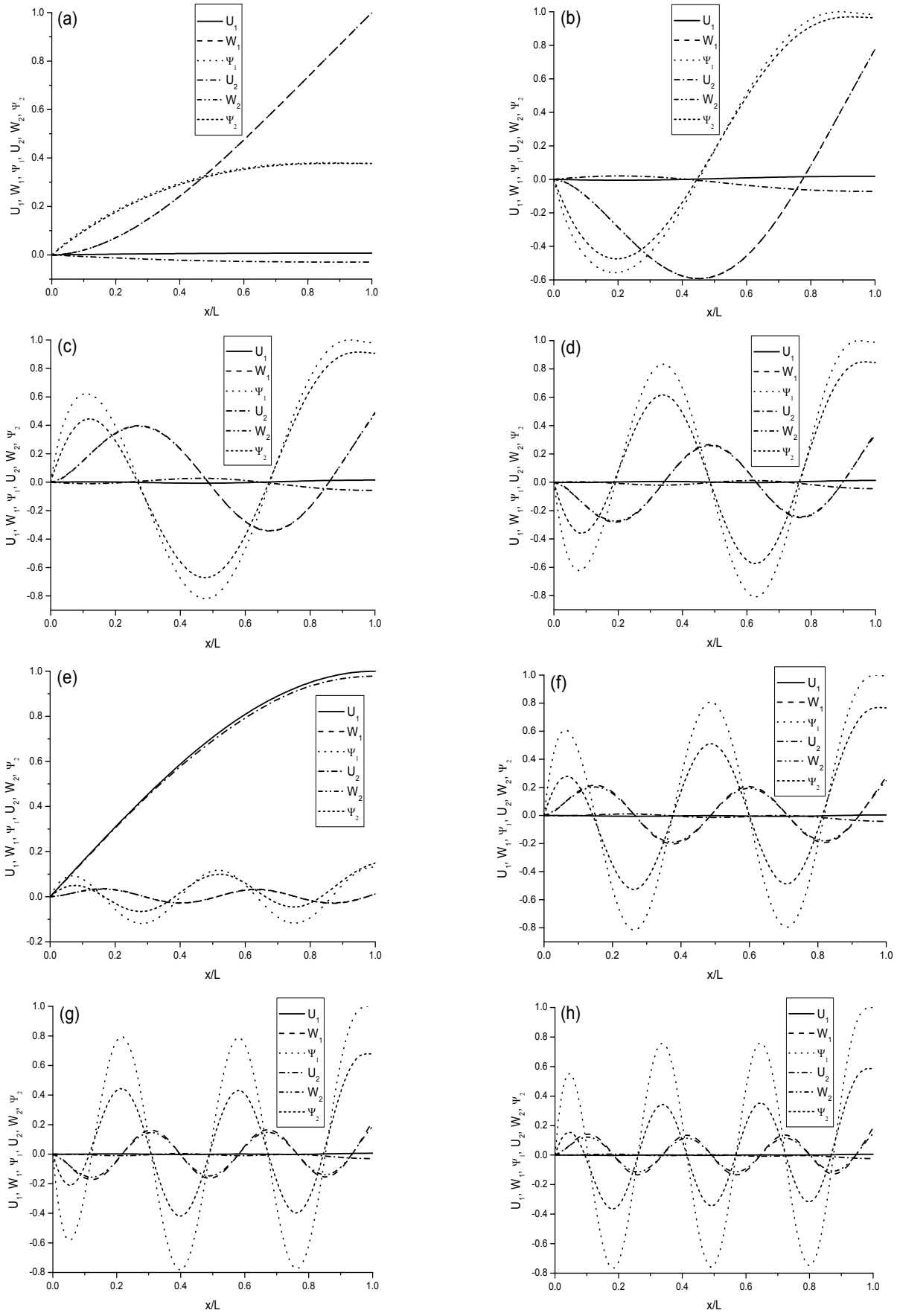

Fig. 4 First fourteenth normal mode shapes of the C-F composite beam: (a) mode 1; (b) mode 2; (c) mode 3; (d) mode 4; (e) mode 5; (f) mode 6; (g) mode 7; (h) mode 8; (i) mode 9; (j) mode 10; (k) mode 11; (l) mode 12; (m) mode 13; (n) mode 14

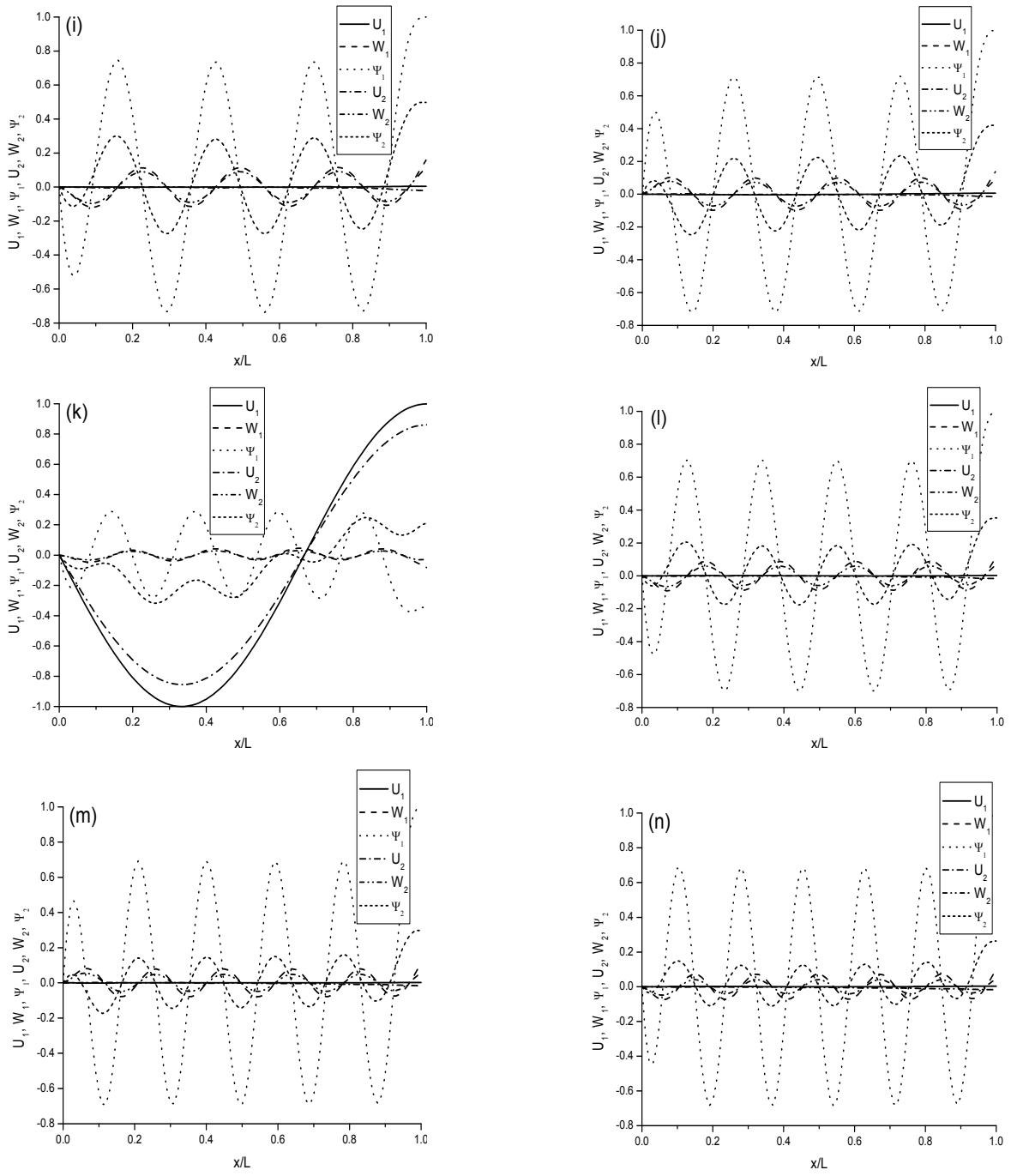

Fig. 4 Continued

steel beam.

The reasonable selection of various parameters is not discussed in detail for the sake of brevity. The geometrical and mechanical properties of the composite beam under study are the same as those used in (Berczynski and Wroblewski 2005), which are characterized by the following parameters

$E_1 = 4.539\times10^{10}\ \mathrm{N/m^2}$, $G_1 = 1.945\times10^{10}\ \mathrm{N/m^2}$,

$A_1 = 3.00\times10^{-2}\ \mathrm{m^2}$, $I_1 = 9.00\times10^{-6}\ \mathrm{m^4}$,

$\rho_1 = 2600\ \mathrm{kg/m^3}$, $k_1 = 1/1.20$, $E_2 = 2.1\times10^{11}\ \mathrm{N/m^2}$,

$G_2 = 8.08\times10^{10}\ \mathrm{N/m^2}$, $A_2 = 1.64\times10^{-3}\ \mathrm{m^2}$,

$I_2 = 5.41\times10^{-6}\ \mathrm{m^4}$, $\rho_2 = 7850\ \mathrm{kg/m^3}$, $k_1 = 1/2.49$,

$L = 3.5\ \mathrm{m}$, $e_c = 0.03\ \mathrm{m}$, $e_s = 0.07\ \mathrm{m}$,

$K = 2.858\times10^{8}\ \mathrm{N/m}$, $E_c = 2.1\times10^{11}\ \mathrm{N/m^2}$,

$A_c = 1.2272\times10^{-4}\ \mathrm{m^2}$, $d = 0.21875\ \mathrm{m}$.

The first fourteen eigenfrequencies of the steel-concrete composite beam with seven end conditions (i.e., C-C, C-H1, C-H2, F-F, C-F, H1-H1 and H2-H2) are computed and the numerical results are displayed in Table 1. The composite

beam is modeled using one element only. To compare the present results with some results available in literature, we also list the analytical solutions obtained in (Berczynski and Wroblewski 2005) and the experimental results given in (Biscontin *et al*. 2000) in Table 1 for the composite beam with F-F end condition. It may be mentioned that the rigid body vibration frequencies are ignored.

Table 1 shows the influence of the end condition on the natural frequencies of the composite beam. An observation of the numerical results shown in Table 1 reveals that the end condition has a significant effect on the natural frequencies of the composite beam. Keeping the mode order invariant, the eigenfrequency of the composite beam with F-F end condition is the highest and that of the composite beam with C-F end condition is the lowest. From the numerical analysis it is seen that there is a general tendency to decrease the natural frequency in the case of increasing fixing extent.

With reference to Table 1, a comparison of the results obtained by the present procedure with those derived by means of the analytical analysis method in (Berczynski and Wroblewski 2005) shows that complete agreement is found for the first eight bending modes. For the first five modes, the eigenfrequencies obtained using the present dynamic stiffness method and the experimental values are in perfect agreement, as can be seen from Table 1. However, when the mode order increases, the bending vibration eigenfrequencies of the composite beam deviate from the experimental results. Both the results achieved by the present formulation and by the analytical method in (Berczynski and Wroblewski 2005) overestimate the eigenfrequencies associated with the bending vibration modes. It can also be observed that the present results are slightly accurate than those given in (Berczynski and Wroblewski 2005) when compared to the experimental values. As far as the longitudinal eigenfrequencies are concerned, the present results are highly consistent with the experimental values for the first two longitudinal vibration modes.

The exact modes of vibration of the C-F composite beam are calculated by the present formulation and are illustrated in Fig. 4. The first fourteen normal mode shapes are plotted in Figs. 4(a)-(n). It can be seen from Fig. 4 that the longitudinal displacement, bending displacement and bending rotation are coupled for all the fourteen mode shapes. In other words, no deformation components equal to zero. It can also be clearly seen that each mode shape is either dominated longitudinal vibration or dominated bending vibration. This is the reason that the terms of longitudinal modes and bending modes are used in this section for the sake of simplicity and unambiguity. For the modes 5 and 11, the longitudinal vibration is prevailed; while for the other modes, the bending vibration is dominated. The differences in the longitudinal displacement between the concrete slab and the steel beam are evident for the first two longitudinal vibration modes. The discrepancies in the longitudinal displacement between the concrete slab and the steel beam are noticeable for the lower bending eigenfrequencies, while these discrepancies become rather small for the higher bending eigenfrequencies. In fact, the coupling between the longitudinal vibration and the bending vibration is rather weak for the higher bending modes. The bending displacements of the concrete slab and the steel beam are hardly distinguished for the first five modes. However, the bending rotations of the concrete slab and the steel beam have significant differences except for the fundamental mode.

In order to better understand the dominated deformation in each mode shape of the C-F composite beam, the percentages of the strain energies stored in the concrete slab, the steel beam, and the connectors are calculated, respectively. The numerical results are displayed in Table 2. The strain energy percents of the concrete slab and the steel beam are composed of three parts including shear, bending and longitudinal strain energy percents, respectively. It can be seen from Table 2 that for the modes 5 and 11, the total longitudinal strain energies stored in the concrete slab and

Table 2 Percentages of strain energies stored in concrete slab, steel beam and connectors of C-F composite beam

Mode No.	Concrete slab			Steel beam			Connectors
	Shear	Bending	Longitudinal	Shear	Bending	Longitudinal	
1	0.02	10.22	11.56	1.76	26.97	45.69	3.79
2	0.12	13.64	6.96	8.60	28.90	27.36	14.42
3	0.24	17.48	4.03	14.23	30.01	15.77	18.24
4	0.41	21.92	2.11	19.07	29.77	8.11	18.61
5	0	0.03	80.25	0.04	0.03	19.54	0.11
6	0.64	26.62	1.11	22.42	27.77	4.33	17.11
7	0.96	31.61	0.58	24.33	24.46	2.26	15.80
8	1.38	36.80	0.33	24.74	20.43	1.24	15.08
9	1.92	42.14	0.19	23.85	16.32	0.70	14.88
10	2.61	47.41	0.27	21.96	12.56	0.38	14.81
11	0	0.07	83.54	0.15	0.02	15.50	0.72
12	3.45	52.55	0.07	19.55	9.42	0.27	14.69
13	4.43	57.20	0.04	16.92	6.93	0.19	14.29
14	5.53	61.18	0.05	14.38	5.05	0.13	13.68

the steel beam contain 99.79% and 99.04% of the total strain energy of the whole composite beam, respectively. That is, the modes 5 and 11 are dominated longitudinal vibration modes, which is consistent with the mode shapes shown in Figs. 4(e) and 4(k).

5. Conclusions

An exact dynamic stiffness matrix capable of accurately analyzing the free vibration of the steel-concrete composite beams is established in this paper. The effects of shear deformation and rotary inertia as well as the relative longitudinal displacement and relative transverse displacement of the two beams are considered in the mathematical model. The dynamic stiffness matrix is developed by directly solving the governing differential equations of motion of the composite beams in free vibration. The application of the dynamic stiffness method is illustrated by evaluating the natural frequencies and mode shapes of an appropriately chosen composite beam with seven end conditions. For the first five bending eigenfrequencies the present results are in perfect agreement with the experimental values. When the mode order increases, the present bending eigenfrequencies slightly deviate from the experimental results. As far as the longitudinal eigenfrequencies are concerned, the present results are highly consistent with the experimental values for the first two longitudinal vibration modes. In addition, the present results are somewhat accurate than the existing solutions when compared to the experimental values. Although the particular example clarified in this paper is a single-span composite beam, the present method can be applied to more general composite beam assemblages without any difficulty.

References

Adam, C., Heuer, R. and Jeschko, A. (1997), "Flexural vibrations of elastic composite beams with interlayer slip", *Acta Mech*., **125**(1), 17-30.

Berczynski, S. and Wroblewski, T. (2005), "Vibration of steel-concrete composite beams using the Timoshenko beam model", *J. Vib. Control*, **11**(6), 829-848.

Berczynski, S. and Wroblewski, T. (2010), "Experimental verification of natural vibration models of steel-concrete composite beams", *J. Vib. Control*, **16**(14), 2057-2081.

Biscontin, G., Morassi, A. and Wendel, P. (2000), "Vibrations of steel-concrete composite beams", *J. Vib. Control*, **6**(5), 691-714.

Dilena, M. and Morassi, A. (2003), "A damage analysis of steel-concrete composite beams via dynamic methods: Part II Analytical models and damage detection", *J. Vib. Control*, **9**(5), 529-565.

Dilena, M. and Morassi, A. (2009), "Vibrations of steel-concrete composite beams with partially degraded connection and applications to damage detection", *J. Sound Vib*., **320**(1), 101-124.

Girhammar, U.A. and Pan, D. (1993), "Dynamic analysis of composite members with interlayer slip", *Int. J. Solids Struct*., **30**(6), 797-823.

Girhammar, U.A., Pan, D.H. and Gustafsson, A. (2009), "Exact dynamic analysis of composite beams with partial interaction", *Int. J. Mech. Sci*., **51**, 565-582.

Henderson, I.E.J., Zhu, X.Q., Uy, B. and Mirza, O. (2015a), "Dynamic behaviour of steel-concrete composite beams with different types of shear connectors. Part I: Experimental study", *Eng. Struct*., **103**, 298-307.

Henderson, I.E.J., Zhu, X.Q., Uy, B. and Mirza, O. (2015b), "Dynamic behaviour of steel-concrete composite beams with different types of shear connectors. Part II: Modelling and comparison", *Eng. Struct*., **103**, 308-317.

Jimbo, S., Morassi, A., Nakamura, G. and Shirota, K. (2012), "A non-destructive method for damage detection in steel-concrete structures based on finite eigendata", *Inverse Probl. Sci. Eng*., **20**(2), 233-270.

Lee, U. (2009), *Spectral Element Method in Structural Dynamics*, John Wiley & Sons, Singapore.

Lenci, S. and Clementi, F. (2012), "Effects of shear stiffness, rotatory and axial inertia, and interface stiffness on free vibrations of a two-layer beam", *J. Sound Vib*., **331**(24), 5247-5267.

Li, J., Huo, Q., Li, X., Kong, X. and Wu, W. (2014), "Dynamic stiffness analysis of steel-concrete composite beams", *Steel Compos. Struct*., *Int. J*., **16**(6), 577-593.

Morassi, A. and Rocchetto, L. (2003), "A damage analysis of steel-concrete composite beams via dynamic methods: Part I Experimental results", *J. Vib. Control*, **9**(5), 507-527.

Morassi, A., Nakamura, G. and Sini, M. (2005), "An inverse dynamical problem for connected beams", *Eur. J. App. Math*., **16**(1), 83-109.

Morassi, A., Nakamura, G., Shirota, K. and Sini, M. (2007), "A variational approach for an inverse dynamical problem for composite beams", *Eur. J. App. Math*., **18**(1), 21-55.

Nguyen, Q.H., Hjiaja, M. and Grognec, P.L. (2012), "Analytical approach for free vibration analysis of two-layer Timoshenko beams with interlayer slip", *J. Sound Vib*., **331**(12), 2949-2961.

Shen, X.D., Chen, W.Q., Wu, Y.F. and Xu, R.Q. (2011), "Dynamic analysis of partial-interaction composite beams", *Compos. Sci. Technol*., **71**(10), 1286-1294.

Wittrick, W.H. and Williams, F.W. (1971), "A general algorithm for computing natural frequencies of elastic structures", *Q. J. Mech. Appl. Math*., **24**(3), 263-284.

Wu, Y.F., Xu, R. and Chen, W. (2007), "Free vibrations of the partial-interaction composite members with axial force", *J. Sound Vib*., **299**(4), 1074-1093.

Xu, R. and Wu, Y. (2007), "Static, dynamic, and buckling analysis of partial interaction composite members using Timoshenko's beam theory", *Int. J. Mech. Sci*., **49**(10), 1139-1155.

Zhou, W., Jiang, L., Huang, Z. and Li, S. (2016), "Flexural natural vibration characteristics of composite beam considering shear deformation and interface slip", *teel Compos. Struct*., *Int. J*., **20**(5), 1023-1042

CC

Appendix

The coefficients η_i ($i = 0 - 6$) in Eq. (12) are

$$\begin{aligned}\eta_0 = &-(a_2a_4(a_4a_8 + 2a_3a_9) + a_{11}(a_4^2a_8 + a_{15}(a_3^2 \\ &- a_2a_8) + 2a_3a_4a_9 + a_2a_9^2) + k(2a_4^2a_8 + 4a_3a_4a_9 \\ &- a_9^2k) + a_{15}(a_2a_3^2 + k(2a_3^2 + a_8k)))(a_{13}a_6 - \mu^2)\end{aligned}$$

$$\begin{aligned}\eta_1 = &-a_{12}^2a_6(a_2a_3^2 + k(2a_3^2 + a_8k)) - a_{13}((a_1 \\ &+ a_{10})a_4a_6(a_4a_8 + 2a_3a_9) + a_2(a_{14}a_3^2a_6 + a_4^2(a_6a_7 \\ &+ a_5(a_5 + a_8)) + 2a_3a_4a_5a_9 + a_{10}a_6a_9^2) + 2(a_{14}a_3^2a_6 \\ &+ a_4^2(a_6a_7 + a_5(a_5 + a_8)) + 2a_3a_4a_5a_9)k + (a_{14}a_6a_8 \\ &- a_5a_9^2)k^2 + a_{15}((a_1 + a_{10})a_3^2a_6 + a_2(a_3^2a_5 - a_{10}a_6a_8) \\ &+ 2a_3^2a_5k + (a_6a_7 + a_5(a_5 + a_8))k^2)) + (a_{10}(a_4^2a_8 \\ &+ a_{15}(a_3^2 - a_2a_8) + 2a_3a_4a_9 + a_2a_9^2) + a_1(a_{15}a_3^2 \\ &+ a_4(a_4a_8 + 2a_3a_9)) + a_7(a_2a_4^2 + k(2a_4^2 + a_{15}k)) \\ &+ a_{14}(a_2a_3^2 + k(2a_3^2 + a_8k)))\mu^2 - a_{11}(a_{12}a_6(a_4^2a_8 \\ &+ a_{12}(a_3^2 - a_2a_8) + a_{15}(a_3^2 - a_2a_8) + 2a_3a_4a_9 + a_2a_9^2) \\ &+ a_{13}(a_{14}a_6(a_3^2 - a_2a_8) + a_4^2(a_6a_7 + a_5(a_5 + a_8)) \\ &+ a_{15}(a_3^2a_5 - a_1a_6a_8 - a_2(a_6a_7 + a_5(a_5 + a_8))) \\ &+ 2a_3a_4a_5a_9 + (a_2a_5 + a_1a_6)a_9^2) + 2a_{12}a_5(a_3a_4 \\ &+ a_2a_9)\mu + (-a_{14}a_3^2 + a_{15}a_2a_7 - a_4^2a_7 + a_1a_{15}a_8 \\ &+ a_{14}a_2a_8 - a_1a_9^2)\mu^2) - a_{12}(a_{15}a_6(a_2a_3^2 + k(2a_3^2 \\ &+ a_8k)) + a_2a_4(a_4a_6a_8 + 2a_3(a_6a_9 + a_5\mu)) \\ &+ k(2a_4^2a_6a_8 + 4a_3a_4(a_6a_9 + a_5\mu) \\ &- a_9k(a_6a_9 + 2a_5\mu)))\end{aligned}$$

$$\begin{aligned}\eta_2 = &-a_{13}a_{14}a_2a_3^2a_5 - a_{13}a_2a_4^2a_5a_7 - 2a_{13}a_{14}a_3^2a_5k \\ &- 2a_{13}a_4^2a_5a_7k - a_{13}a_{14}a_5^2k^2 - a_{13}a_{15}a_5a_7k^2 \\ &- a_{13}a_{14}a_6a_7k^2 - a_{13}a_{14}a_5a_8k^2 - a_{12}^2(a_2a_3^2a_5 \\ &+ k(2a_3^2a_5 + (a_6a_7 + a_5(a_5 + a_8))k))\end{aligned}$$

The coefficients t_j, $\bar{t}_j$, $\hat{t}_j$, $\tilde{t}_j$ and $\breve{t}_j$ ($j = 1 - 6$) in Eqs. (15a)-(15e) are

$$\begin{aligned}\eta_3 = &\, a_{11}(a_{12}^2a_2a_5a_7 + a_{13}a_{14}a_2a_5a_7 + a_{12}((a_{15}a_2 \\ &- a_4^2)a_5a_7 + a_{14}(-a_3^2a_5 + a_2(a_6a_7 + a_5(a_5 + a_8))))) \\ &- a_{12}^2a_5a_7k^2 - a_{13}a_{14}a_5a_7k^2 - a_{12}(a_5a_7(a_2a_4^2 + k(2a_4^2 \\ &+ a_{15}k)) + a_{14}(a_2a_3^2a_5 + k(2a_3^2a_5 + (a_6a_7 + a_5(a_5 \\ &+ a_8))k))) + a_{10}(a_{12}^2(-a_3^2a_5 + a_2(a_6a_7 + a_5(a_5 \\ &+ a_8))) + a_{13}((a_{15}a_2 - a_4^2)a_5a_7 + a_{14}(-a_3^2a_5 + a_2(a_6a_7 \\ &+ a_5(a_5 + a_8)))) - a_{12}(a_{14}a_6(a_3^2 - a_2a_8) + a_4^2(a_6a_7 \\ &+ a_5(a_5 + a_8)) + a_{15}(a_3^2a_5 - a_2(a_6a_7 + a_5(a_5 + a_8))) \\ &+ 2a_3a_4a_5a_9 + a_2a_5a_9^2) - a_{14}a_2a_7\mu^2) + a_1(a_{12}^2(-a_3^2a_5 \\ &+ a_{10}a_6a_8 + a_{11}(a_6a_7 + a_5(a_5 + a_8))) + a_{13}((a_{11}a_{15} \\ &- a_4^2)a_5a_7 + a_{14}(-a_3^2a_5 + a_{10}a_6a_8 + a_{11}(a_6a_7 + a_5(a_5 \\ &+ a_8))) + a_{10}(a_{15}(a_6a_7 + a_5(a_5 + a_8)) - a_5a_9^2)) \\ &- (a_{11}a_{14}a_7 + a_{10}a_{15}a_7 + a_{10}a_{14}a_8)\mu^2 - a_{12}(a_{14}a_6(a_3^2 \\ &- a_{11}a_8) + a_4^2(a_6a_7 + a_5(a_5 + a_8)) + a_{15}(a_3^2a_5 \\ &- a_{10}a_6a_8 - a_{11}(a_6a_7 + a_5(a_5 + a_8))) + 2a_3a_4a_5a_9 \\ &+ a_9(a_{11}a_5a_9 + a_{10}a_6a_9 + 2a_{10}a_5\mu)))\end{aligned}$$

$$\begin{aligned}\eta_4 = &\, a_{10}(a_{12}^2a_2a_5a_7 + a_{13}a_{14}a_2a_5a_7 + a_{12}((a_{15}a_2 \\ &- a_4^2)a_5a_7 + a_{14}(-a_3^2a_5 + a_2(a_6a_7 + a_5(a_5 + a_8))))) \\ &+ a_{12}a_{14}a_5a_7(a_{11}a_2 - k^2) + a_1(a_{11}a_{13}a_{14}a_5a_7 \\ &+ a_{12}^2(a_{11}a_5a_7 + a_{10}(a_6a_7 + a_5(a_5 + a_8))) \\ &+ a_{12}((a_{11}a_{15} - a_4^2)a_5a_7 + a_{14}(-a_3^2a_5 + a_{10}a_6a_8 \\ &+ a_{11}(a_6a_7 + a_5(a_5 + a_8))) + a_{10}(a_{15}(a_6a_7 \\ &+ a_5(a_5 + a_8)) - a_5a_9^2)) + a_{10}(a_{13}(a_{15}a_5a_7 \\ &+ a_{14}(a_6a_7 + a_5(a_5 + a_8))) - a_{14}a_7\mu^2))\end{aligned}$$

$$\begin{aligned}\eta_5 = &\, a_{10}a_{12}a_{14}a_2a_5a_7 + a_1(a_{11}a_{12}a_{14}a_5a_7 \\ &+ a_{10}(a_{12}^2a_5a_7 + a_{13}a_{14}a_5a_7 + a_{12}(a_{15}a_5a_7 + a_{14}(a_6a_7 \\ &+ a_5(a_5 + a_8)))))\end{aligned}$$

$$\begin{aligned}t_j = &((a_{11} + k + a_{10}\kappa_j^2)(-(a_{13} + a_{12}\kappa_j^2)(a_3a_9(a_6 \\ &+ a_5\kappa_j^2) + a_4(a_6(a_8 + a_7\kappa_j^2) + a_5\kappa_j^2(a_5 + a_8 \\ &+ a_7\kappa_j^2))) - a_{12}a_3a_5\kappa_j^2\mu + (a_3a_9 + a_4(a_8 \\ &+ a_7\kappa_j^2))\mu^2))\big/\kappa_j\Delta_j\end{aligned}$$

$$\begin{aligned}\bar{t}_j = &((a_{13} + a_{12}\kappa_j^2)(a_6 + a_5\kappa_j^2)(a_{11}a_3a_4 + a_2a_3a_4 \\ &+ a_{11}a_2a_9 + 2a_3a_4k - a_9k^2 + ((a_1 + a_{10})a_3a_4 \\ &+ (a_1a_{11} + a_{10}a_2)a_9)\kappa_j^2 + a_1a_{10}a_9\kappa_j^4) + a_{12}a_5\kappa_j^2(-k^2 \\ &+ (a_2 + a_1\kappa_j^2)(a_{11} + a_{10}\kappa_j^2))\mu - (a_{11}a_3a_4 + a_2a_3a_4 \\ &+ a_{11}a_2a_9 + 2a_3a_4k - a_9k^2 + ((a_1 + a_{10})a_3a_4 \\ &+ (a_1a_{11} + a_{10}a_2)a_9)\kappa_j^2 + a_1a_{10}a_9\kappa_j^4)\mu^2)\big/\kappa_j\Delta_j\end{aligned}$$

$$\begin{aligned}\hat{t}_j = &((a_2 + k + a_1\kappa_j^2)((a_{13} + a_{12}\kappa_j^2)(a_3a_9(a_6 + a_5\kappa_j^2) \\ &+ a_4(a_6(a_8 + a_7\kappa_j^2) + a_5\kappa_j^2(a_5 + a_8 + a_7\kappa_j^2))) \\ &+ a_{12}a_3a_5\kappa_j^2\mu - (a_3a_9 + a_4(a_8 + a_7\kappa_j^2))\mu^2))\big/\kappa_j\Delta_j\end{aligned}$$

$$\begin{aligned}\tilde{t}_j = &(-a_{12}(a_3^2(2k + (a_1 + a_{10})\kappa_j^2)(a_6 + a_5\kappa_j^2) \\ &+ (k^2 - a_1a_{10}\kappa_j^4)(a_6(a_8 + a_7\kappa_j^2) + a_5\kappa_j^2(a_5 + a_8 \\ &+ a_7\kappa_j^2)) + a_2(a_3^2(a_6 + a_5\kappa_j^2) - a_{10}\kappa_j^2(a_6(a_8 \\ &+ a_7\kappa_j^2) + a_5\kappa_j^2(a_5 + a_8 + a_7\kappa_j^2)))) - a_5(-a_9k^2 \\ &+ a_1a_{10}a_9\kappa_j^4 + a_3a_4(2k + (a_1 + a_{10})\kappa_j^2) + a_2(a_3a_4 \\ &+ a_{10}a_9\kappa_j^2))\mu + a_{11}(a_{12}(-a_3^2(a_6 + a_5\kappa_j^2) + (a_2 \\ &+ a_1\kappa_j^2)(a_6(a_8 + a_7\kappa_j^2) + a_5\kappa_j^2(a_5 + a_8 + a_7\kappa_j^2))) \\ &- a_5(a_3a_4 + a_9(a_2 + a_1\kappa_j^2))\mu))\big/\Delta_j\end{aligned}$$

$$\breve{t}_j = (-a_{13}(a_3^2(2k + (a_1 + a_{10})\kappa_j^2)(a_6 + a_5\kappa_j^2) + (k^2 - a_1 a_{10}\kappa_j^4)(a_6(a_8 + a_7\kappa_j^2) + a_5\kappa_j^2(a_5 + a_8 + a_7\kappa_j^2)) + a_2(a_3^2(a_6 + a_5\kappa_j^2) - a_{10}\kappa_j^2(a_6(a_8 + a_7\kappa_j^2) + a_5\kappa_j^2(a_5 + a_8 + a_7\kappa_j^2)))) - a_{12}\kappa_j^2(a_3^2(2k + (a_1 + a_{10})\kappa_j^2)(a_6 + a_5\kappa_j^2) + (k^2 - a_1 a_{10}\kappa_j^4)(a_6(a_8 + a_7\kappa_j^2) + a_5\kappa_j^2(a_5 + a_8 + a_7\kappa_j^2)) + a_2(a_3^2(a_6 + a_5\kappa_j^2) - a_{10}\kappa_j^2(a_6(a_8 + a_7\kappa_j^2) + a_5\kappa_j^2(a_5 + a_8 + a_7\kappa_j^2)))) + (a_3^2(2k + (a_1 + a_{10})\kappa_j^2) + (a_8 + a_7\kappa_j^2)(k^2 - a_1 a_{10}\kappa_j^4) + a_2(a_3^2 - a_{10}\kappa_j^2(a_8 + a_7\kappa_j^2)))\mu^2 + a_{11}(a_{13}(-a_3^2(a_6 + a_5\kappa_j^2) + (a_2 + a_1\kappa_j^2)(a_6(a_8 + a_7\kappa_j^2) + a_5\kappa_j^2(a_5 + a_8 + a_7\kappa_j^2))) + a_{12}\kappa_j^2(-a_3^2(a_6 + a_5\kappa_j^2) + (a_2 + a_1\kappa_j^2)(a_6(a_8 + a_7\kappa_j^2) + a_5\kappa_j^2(a_5 + a_8 + a_7\kappa_j^2))) + (a_3^2 - (a_2 + a_1\kappa_j^2)(a_8 + a_7\kappa_j^2))\mu^2))\big/\kappa_j\Delta_j$$

$$\Delta_j = (a_5(a_{13} + a_{12}\kappa_j^2)(k(2a_3a_4 - a_9k) + (a_1 + a_{10})a_3a_4\kappa_j^2 + a_1a_{10}a_9\kappa_j^4 + a_2(a_3a_4 + a_{10}a_9\kappa_j^2)) + a_{12}(a_3^2(2k + (a_1 + a_{10})\kappa_j^2) + (a_8 + a_7\kappa_j^2)(k^2 - a_1a_{10}\kappa_j^4) + a_2(a_3^2 - a_{10}\kappa_j^2(a_8 + a_7\kappa_j^2)))\mu + a_{11}(a_{13}a_5(a_3a_4 + a_9(a_2 + a_1\kappa_j^2)) + a_{12}(a_3a_4a_5\kappa_j^2 + a_3^2\mu + (a_2 + a_1\kappa_j^2)(a_5a_9\kappa_j^2 - (a_8 + a_7\kappa_j^2)\mu))))$$